

Diffusive and structural properties in a binary mixture of charged particles

Wei Kong

*Physics Department, Nankai University, Tianjin, 300071 China
and Physics Department, Auburn University, Auburn, Alabama, 36832 USA*

Songfen Liu* and Beilai Hu

Physics Department, Nankai University, Tianjin, 300071 China

Long Wang

Institute of Physics, The Chinese Academy of Sciences, Beijing, 100080 China

(Received 10 January 2009; revised manuscript received 19 August 2009; published 24 September 2009)

Diffusive and structural properties in the binary mixture of charged particles are investigated based on the molecular dynamical simulation. It is shown that the particles with higher charge enhance or weaken the diffusion of the whole system depending on the coupling strength, and regimes of subdiffusion as well as normal diffusion are identified. The nonmonotonous diffusion, i.e., the diffusion at first is increased and then is decreased with increasing the higher charged particles, is strongest close to the phase from liquidlike state to solidlike state. Stronger coupling and lower concentration of higher charged particles are in favor of the formation of ordered shells centered at the higher charged particles.

DOI: [10.1103/PhysRevE.80.036406](https://doi.org/10.1103/PhysRevE.80.036406)

PACS number(s): 52.27.Lw, 52.35.Fp

I. INTRODUCTION

For a long time the one-component plasmas and one-component colloid suspensions are the good candidates to study many-body systems because of simplification of the complicated objects [1–3]. In many cases, however, the realistic systems are not composed of one component due to many factors [4]. More and more attentions [5–16] are shifted to the multicomponent systems in order to well understand the real physics. In this work we focus on the diffusion and structure in a quasi-two-dimensional (Q2D) binary mixture of charged particles using the molecular dynamical simulation.

The diffusion has been a subject of active research and wide interest for many years. Recently it is becoming attractive to study the interaction of particles in the binary mixture [17–19], in which the properties of system including diffusion behavior, are modified in several ways by the addition of a second component. In general, it is believed that the modification arises from the depletion forces induced by the presence of the second component in the system, and the mechanism is described first by Oosawa and Asakura [20]. Experimentally, colloid particles are becoming useful model system to study the diffusion behavior for the advances in dynamic light scattering methodology and the development of digital imaging technology. More recently, studies of Q2D binary colloid particles [21] show that the diffusion with character of nonmonotonous occurs with addition of the second component, where the nonmonotonous diffusion means addition of a small amount of small diameter particles enhances the diffusion of the system, while further addition of the small diameter particles generates a decrease of the diffusion. This result motivates us to continue studying the dif-

fusion in the binary mixture of charged particles. In this paper, we investigate the dependence of diffusion on the coupling of system and concentration of higher charged particles, which is different from the most early works that are focused on the colloid particles, in which the sampled parameters mainly are colloid particle diameter ratio, large particle density and small particle fraction. It is found that the nonmonotonous diffusion depends on the coupling of system and is strongest close to the phase transition from liquidlike state to solidlike state, and regimes of subdiffusion as well as normal diffusion are identified in the nonmonotonous diffusion, respectively. Also we have noticed the recent studies on the structural properties of multicomponent system [5–9], which revealed a rich variety of ordered structure can be formed with specific type of interacting forces as well as confined potential, and the structure often depends on the parameters such as competition of short-range and long-range potentials, mass-to-charge ratio, total number particles, and number ratio of the species of particles. Here we show that the formation of ordered shells centered at the higher charged particle depends on the strength of coupling and concentration of higher charged particles. The paper is arranged as follows. In Sec. II, we give a detailed account of the physical model used in our simulation. The results and analysis are presented in Sec. III. Section IV is devoted to a conclusion.

II. BINARY MIXTURE MODEL

We consider a monolayer of interacting charged particles. In order to investigate the effect of higher charged particles on the whole system, we mix the higher charged particles into the background charged particles uniformly before performing the simulations. The higher charged particles are increased gradually by $\eta=1\%$, where η refers to the number fraction of higher charged particles, i.e., $\eta=n/N$. n and N are

*lsfnku@nankai.edu.cn

the number of higher charged particles and whole particles, respectively. For distinguishing the higher charged particles from the background charged particles, we assume the charge and mass of background particles are Q_0 and M_0 respectively. A dimensionless parameter $\mu = Q/Q_0 = M/M_0$ is used to represent the particles with higher charge, for convenience, the charge varies in proportion to the mass. In real condition, the different magnitude of mass of the charged particles may introduce a slight separation of particles on the vertical direction relative to 2D simulation plane, to our consideration, the periodic condition is applied on the 2D plane and the motion of particles along the plane normal is ignored. We employ the term Q2D to differ our system from the standard two-dimensional case. The screened Coulomb potential (Yukawa potential) is used to describe the interaction potential among the charged particles, which is written as $\phi(r) = \frac{Q_i Q_j}{r} e^{-\kappa r}$ for two charged particles (Q_i and Q_j) separated by a distance r . The cutoff distance during calculating the interaction potential among charged particles is supposed to be $L/2$, where L is the side length of the simulation box. The thermodynamics of the screened Coulomb system is characterized by two parameters, coupling constant $\Gamma = Q_i Q_j / (4\pi\epsilon_0 a T)$ and screening constant $\kappa = a/\lambda_D$, where Γ is the ratio of Coulomb interaction energy to the kinetic energy. In our simulation, Γ ranges from 2.5 to 500, which suggests gaslike, liquidlike, and solidlike states are all considered in the study. It has been reported that the melting temperature corresponds a value of $\Gamma = 142.9$ when $\kappa = 1$ [22], here we choose $\kappa = 1$ to represent the real experimental condition. Units are applied, length is in the unit of the mean interparticle distance a , energy is in the unit of $U_0 = Q_0^2 / (4\pi\epsilon_0 a)$ and time is in the unit of $t_0 = \sqrt{4\pi\epsilon_0 M_0 a^3 / Q_0^2} = \sqrt{4\pi\omega_{pd}^{-1}}$ (ω_{pd} is the plasma frequency). The random force from the heat bath is adjusted before computing the characteristic functions and Nosé-Hoover thermostat scheme [23] is applied to achieve the constant temperature. In each computing, we have made sure the system being in the equilibrium by adjusting the damping coefficient. As shown in Fig. 1, we present an example of the fluctuation of kinetic energy for the long run time (the first 5×10^4 steps for achieving the system equilibrium, and the subsequent 3×10^4 steps for calculating the characteristic functions), which shows the fluctuation of kinetic energy is around 2%. We use $N=900$ and $N=1600$ to perform the simulations and get the consistent results.

III. SIMULATION RESULTS AND ANALYSIS

Three characteristic functions, mean-squared displacement (MSD), self-diffusion coefficient [$D(t)$] and velocity-autocorrelation function (VACF), are used to account for the simulation results. We begin with MSD, which is defined by

$$\langle r^2(t) \rangle = \left\langle \frac{1}{N} \sum_{i=1}^N [\vec{r}_i(t) - \vec{r}_i(0)]^2 \right\rangle. \quad (1)$$

It is known that MSD is useful in providing the diffusion information. we choose two typical Γ to show the effects of coupling on the diffusion. In Fig. 2(a), for the case of Γ

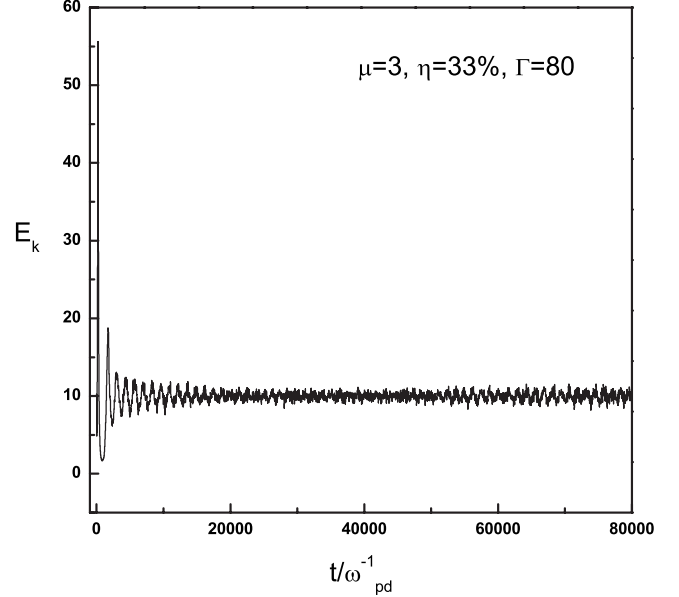


FIG. 1. Kinetic energy fluctuates with time.

$=40$ (corresponding to the liquidlike state), the MSD curves descend continuously with increasing η . However, the curves take a different appearance when Γ is increased, for the case of $\Gamma=120$ (corresponding to the liquid-to-solid state) as shown in Fig. 2(b), MSD curves first mount up with increasing η and reach the maximum when $\eta \approx 4\%$, with further increasing η , MSD curves turn to descend even lower than that of $\eta=0$. In Figs. 2(c) and 2(d), we continue to give the dependence of $D(t)$ on η for the cases of $\Gamma=40$ and $\Gamma=120$, respectively, where $D(t)$ is determined by the Einstein relation [24] if the trajectories of the moving particles are resolved,

$$D(t) = \lim_{t \rightarrow \infty} \frac{\langle r^2(t) \rangle}{4t}. \quad (2)$$

One can see the results agreed with that of left part of Fig. 2. Specially in Fig. 2(d), $D(t)$ decreases with further increasing the higher charged particles, even less than $D(t)$ of $\eta=0$. The key results of Fig. 2 are as follows.

(1) The nonmonotonous diffusion varying with η occurs for a wide range of Γ and is strongest close to the phase from liquidlike state to solidlike state, as shown in Fig. 5.

(2) For the nonmonotonous diffusion, there is a particular value of η_{\max} , which divides the diffusion from increased to decreased. It is reasonable to expect η_{\max} to increase when μ is decreased, as shown in Fig. 5.

(3) In the nonmonotonous diffusion, as shown in Fig. 2(d), there is a big gap between the maximum $D(t)$ and the minimum $D(t)$, as large as one order of magnitude, which suggests the existence of different regimes of diffusion. Further increasing the higher charged particles will increase the gap.

(4) The cutoff distance may has an important effect on the nonmonotonous diffusion, we have performed the simulations with two other cutoff distances, $2L/3$ and $3L/4$. As shown in the Fig. 2(d), the peaks of $D(t)$ nearly overlap each

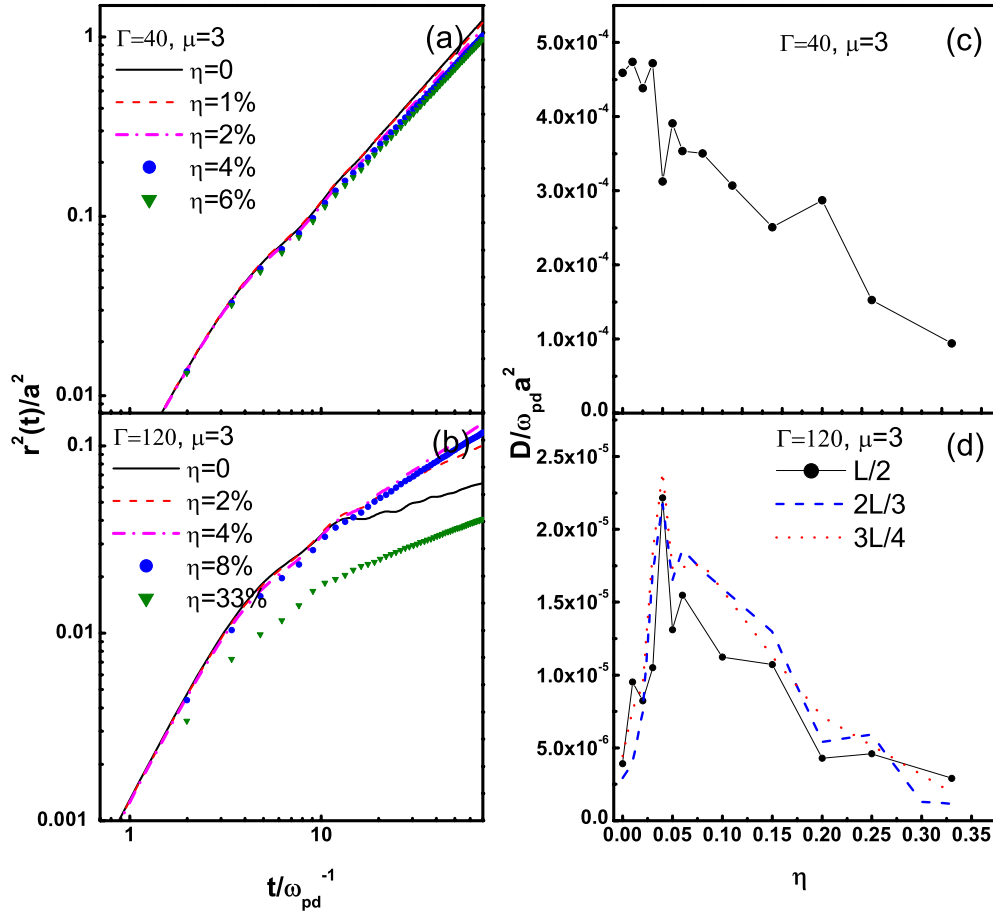


FIG. 2. (Color online) [(a) and (b)] Mean-squared displacement vs time on the log-log plot. [(c) and (d)] Self-diffusion coefficient $D(t)$ vs number fraction of higher charged particles η . $D(t)$ is calculated for a long time $\omega_{pd}t=200$. For $\Gamma=40$, increasing the higher charged particles leads to a monotonic decrease in MSD and $D(t)$. For $\Gamma=120$, MSD and $D(t)$ exhibit the nonmonotonous character with increasing the higher charged particles. In panel (d), which shows the nonmonotonous diffusion with three different cutoff distances, $L/2$ and $3L/4$.

other. With the cutoff distance of $L/2$, it is accurate enough to describe our main results (the dependence of nonmonotonous diffusion on η). We adopt the cutoff distance of $L/2$ in order to save the computation time.

As mentioned above, the value of $D(t)$ changes remarkably with η for the higher Γ , which suggests the transition among subdiffusion, normal diffusion, and superdiffusion may happen. Here we are about to show the transition between subdiffusion and normal diffusion with increasing the higher charged particles under a set of plasmas parameters: $\kappa=1$, $\Gamma=100$, and $\mu=3$. According to the prescription of Feder *et al.* [25]: a range of $0.1 < \alpha < 0.9$ is an anomalous subdiffusion, the range of $0.9 < \alpha < 1.1$ is classified as normal diffusion and superdiffusion appears when $\alpha > 1.1$, where α is the characteristic slope

$$\alpha = \frac{d[\log\langle(\vec{r}_i(t) - \vec{r}_i(0))^2\rangle]}{d[\log t]} \quad (3)$$

We average the value of α in the range of $35 < \omega_{pd}t < 80$ as shown in Fig. 3 and find that with increasing the higher

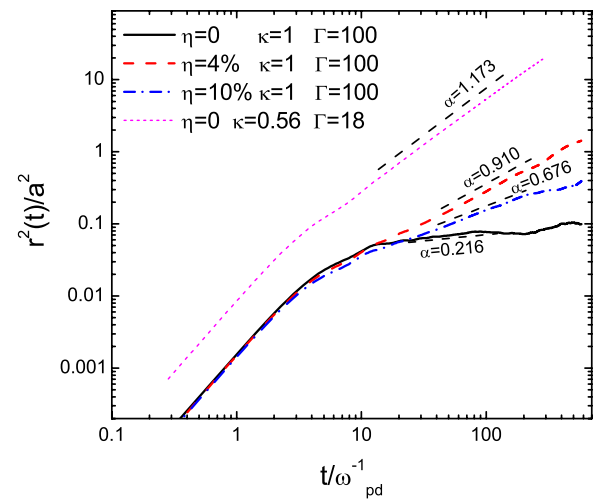


FIG. 3. (Color online) Mean-squared displacement vs time on the log-log plot. The slopes are calculated at later times ($35 < \omega_{pd}t < 80$). It shows the subdiffusion ($\alpha=0.216$) changes to the normal diffusion ($\alpha=0.910$) with increasing higher charged particles. The superdiffusion ($\alpha=1.173$) occurs for the parameters of $\eta=0$, $\kappa=0.56$, and $\Gamma=18$.

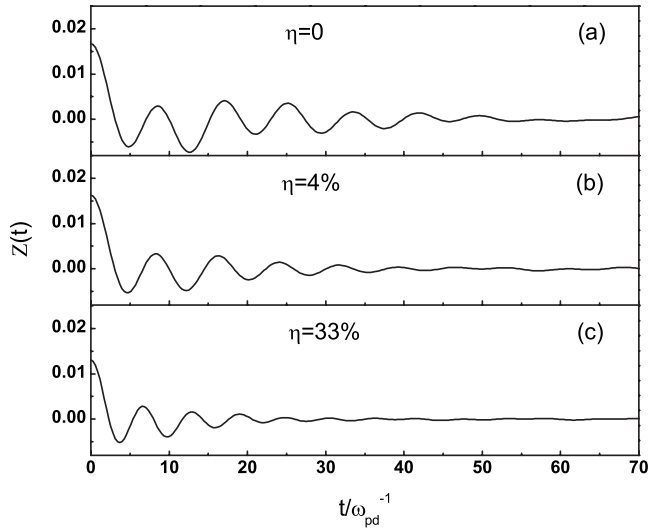


FIG. 4. Velocity autocorrelation function vs time for $\Gamma=120$. The oscillation of VACF becomes weak with increasing the higher charged particles.

charged particles, α is increased from 0.216 ($\eta=0$) to 0.910 ($\eta=4\%$), which indicates the transition from subdiffusion to normal diffusion happens. With further increasing higher charged particles, α is decreased to 0.676 ($\eta=10\%$). We continue to investigate the diffusion over a wide range of Γ (2.5–400) and find no superdiffusion in the case discussed. Liu and Goree [1] have reported the regime of superdiffusion in the liquids with the value of $\kappa=0.56$, we reproduce their results with $\kappa=0.56$, $\eta=0$, and $\Gamma=18$, as shown in Fig. 3.

VACF is another widely used function to character the collective motion of the particles, which is defined by

$$Z(t) = \frac{\left\langle \sum_{i=1}^N \vec{v}_i(t) \cdot \vec{v}_i(0) \right\rangle}{\left\langle \sum_{i=1}^N \vec{v}_i(0) \cdot \vec{v}_i(0) \right\rangle}. \quad (4)$$

We employ it to illustrate the collective motion of the system containing higher charged particles. For the higher Γ , the motion of single-particle couples strongly with the collective motion of particles, as indicated in Fig. 4(a), VACF oscillates for a long time when $\eta=0$. While with increasing η , VACF decays quickly, as shown in Figs. 4(b) and 4(c), which means the higher charged particles have an important effect on the dynamical properties of the system and lead to the decoupling between single-particle motion and collective motion. It has been reported that in the intermediate temperature regime, the VACF decays as slowly as $1/t$ and a long-time tail of VACF in log-log axes indicates superdiffusion [2], here the VACF decays much faster than $1/t$ with increasing the higher charged particles, which again verifies the motion is nonsuperdiffusive.

Figure 5 shows the dependence of η_{\max} on Γ over a wide range (2.5–500, including gaslike state, liquidlike state, and solidlike state). Obviously one can see the nonmonotonous diffusion occurs through a wide range of Γ and is strongest close to the phase from liquidlike state to solidlike state. When $\mu=3$ is decreased to $\mu=2$, as shown in the Fig. 5(a), the range of Γ for the nonmonotonous diffusion is extended slightly, meanwhile, η_{\max} is increased.

Recent studies on the 2D system [5–9] have revealed that the multicomponent charged particles can organize themselves into ordered structures with specific interaction potentials. As referred by Liu *et al.* [5], the stationary ground-state particle ordering is determined by minimizing the total en-

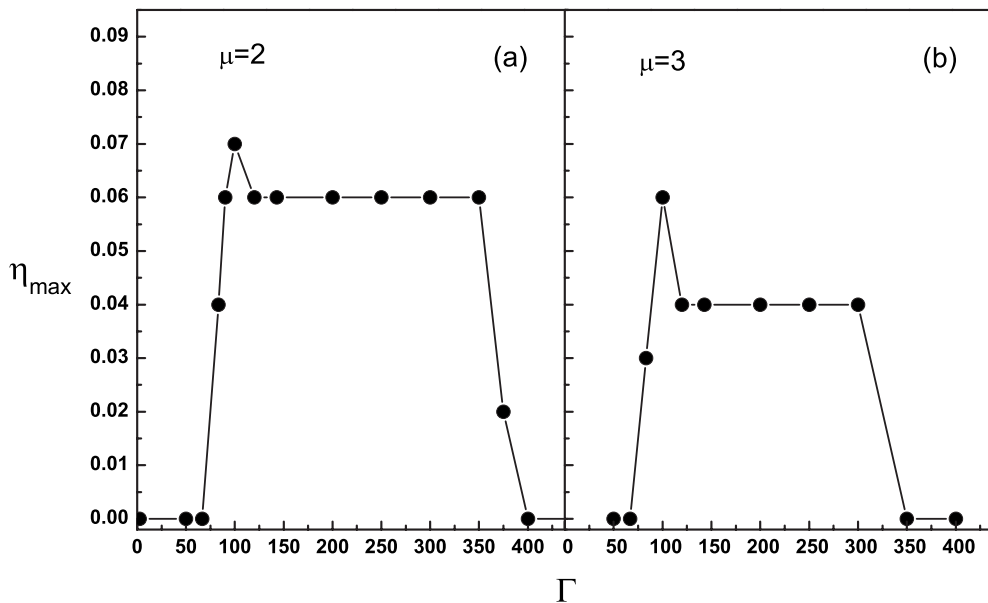


FIG. 5. Dependence of η_{\max} on Γ . With decreasing μ , the range of Γ for η_{\max} is extended slightly, meanwhile, η_{\max} is increased. The nonmonotonous diffusion is strongest close to the phase from liquidlike state to solidlike state.

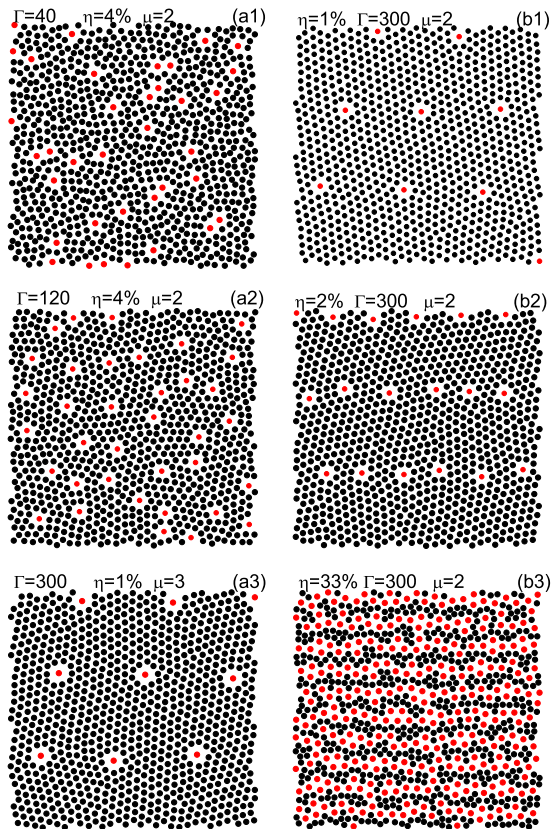


FIG. 6. (Color online) The configuration for binary mixture of charged particles. Total number of the charged particles is 900. a1, a2, and a3 correspond to the cases of $\Gamma=40$, 120, and 300, respectively. b1, b2, and b3 show the configurations of $\eta=1\%$, 2% , and 33% , respectively (red dots indicate the higher charged particles).

ergy of system. Here we show the stationary configuration of binary charged particles under the screened Coulomb potential. The ordered shells centered at the higher charged particles has a strong dependence on the parameters of Γ , η and μ . Figures 6(a2) and 6(a3) show that the ordered shells with certain number of nearest-neighbor particle emerge when the system coupling is strong enough. We have performed many simulations (not shown) with higher Γ and found that the number of nearest-neighbor particle of higher charged particles basically keeps 8, and the number of nearest-neighbor particle of background particles keeps 6 around $\Gamma \geq 150$,

which suggests such configuration in the binary mixture of charged particles undergoes the minimum total energy. Note that when the μ is increased to 3, as shown in Fig. 6(a3), the number of nearest-neighbor particle is 9 or 10, which arises from the stronger repulsion of the higher charged particles. Figures 6(b1)–6(b3) show the ordered shells are destroyed when increasing η too much, as shown in Fig. 6(b3), the background charged particles are pushed into patches, which suggests the phase separation of higher charged particles and background charged particles may occur.

IV. CONCLUSION

The diffusive and structural properties in the binary mixture of charged particles is studied using the molecular dynamical method and the nonmonotonous diffusion is emphasized. We find that the nonmonotonous diffusion has a dependence on the coupling of system, which is strongest close to the phase from liquidlike state to solidlike state. In the early work, Cui *et al.* [26] attribute the initial increase of diffusion generated by addition of a small amount of colloid particles to redistribution of subpopulations of locally ordered and locally disordered domains in the liquid. Here we suggest the higher charged particles generate the similar effects on the binary mixture of charged particles, so it is easy to understand why the strongest nonmonotonous diffusion is close to the phase from liquidlike state to solidlike state (where the particles often exhibit dynamical and structural heterogeneity). For the extreme values of Γ , the redistribution of subpopulations of locally ordered and locally disordered domains are hard to be formed because of quick moving particles (for the very low Γ) or strong interaction among particles (for the very high Γ), respectively. The regimes of subdiffusion as well as normal diffusion are identified in the nonmonotonous diffusion. The shells centered at the higher charged particles are observed, which are subject to the coupling of system, number fraction of higher charged particles and charge magnitude of higher charged particles.

ACKNOWLEDGMENTS

This work was supported by the Ministry of Science and Technology of China, Grant No. 2009GB105000, and the National Science Foundation of China, Grant No. 10547121.

-
- [1] B. Liu, J. Goree, and O. S. Vaulina, *Phys. Rev. Lett.* **96**, 015005 (2006).
 - [2] B. Liu and J. Goree, *Phys. Rev. E* **75**, 016405 (2007).
 - [3] C. C. Grimes and G. Adams, *Phys. Rev. Lett.* **42**, 795 (1979).
 - [4] Y. N. Nejoh, *Phys. Plasmas* **4**, 2813 (1997).
 - [5] Y. H. Liu, Z. Y. Chen, M. Y. Yu, L. Wang, and A. Bogaerts, *Phys. Rev. E* **73**, 047402 (2006).
 - [6] Y. H. Liu, L. Y. Chew, and M. Y. Yu, *Phys. Rev. E* **78**, 066405 (2008).
 - [7] W. Yang, M. Kong, M. V. Milošević, Zhi Zeng, and F. M. Peeters, *Phys. Rev. E* **76**, 041404 (2007).
 - [8] W. P. Ferreira, J. C. N. Carvalho, P. W. S. Oliveira, G. A. Farias, and F. M. Peeters, *Phys. Rev. B* **77**, 014112 (2008).
 - [9] K. Nelissen, B. Partoens, and F. M. Peeters, *Phys. Rev. E* **71**, 066204 (2005).
 - [10] K. Nelissen, B. Partoens, and F. M. Peeters, *Europhys. Lett.* **79**, 66001 (2007).
 - [11] J. A. Drocco, C. J. Olson Reichhardt, C. Reichhardt, and B. Jankó, *Phys. Rev. E* **68**, 060401(R) (2003).
 - [12] K. Nelissen, B. Partoens, and F. M. Peeters, *Phys. Rev. E* **69**,

- 046605 (2004).
- [13] W. P. Ferreira, F. F. Munarin, K. Nelissen, R. N. Costa Filho, F. M. Peeters, and G. A. Farias, *Phys. Rev. E* **72**, 021406 (2005).
- [14] B. A. Grzybowski, X. Jiang, H. A. Stone, and G. M. Whitesides, *Phys. Rev. E* **64**, 011603 (2001).
- [15] D. T. Valley, S. A. Rice, B. Cui, H. M. Ho, H. Diamant, and B. Lin, *J. Chem. Phys.* **126**, 134908 (2007).
- [16] W. Kong, S. F. Liu, Q. L. Wang, B. L. Hu, and L. Wang, *J. Phys. A: Math. Theor.* **40**, 1171 (2007).
- [17] B. Götzelmann, R. Evans, and S. Dietrich, *Phys. Rev. E* **57**, 6785 (1998).
- [18] J. M. Méndez-Alcaraz and R. Klein, *Phys. Rev. E* **61**, 4095 (2000).
- [19] P. Nikunen, I. Vattulainen, and T. Ala-Nissila, *J. Chem. Phys.* **117**, 6757 (2002).
- [20] F. Oosawa and S. Asakura, *J. Chem. Phys.* **22**, 1255 (1954).
- [21] H. M. Ho, B. Cui, S. Repel, B. Lin, and S. A. Rice, *J. Chem. Phys.* **121**, 8627 (2004).
- [22] B. Liu, Y. H. Liu, Y. P. Chen, S. Z. Yang, and L. Wang, *Chin. Phys.* **12**, 765 (2003).
- [23] W. G. Hoover, *Phys. Rev. A* **31**, 1695 (1985).
- [24] H. Gould and J. Tobochnik, *An Introduction to Computer Simulation Methods* (Addison-Wesley, Reading, MA, 1988), Vol. i.
- [25] T. J. Feder, I. Brust-Mascher, J. P. Slattery, B. Baird, and W. W. Webb, *Biophys. J.* **70**, 2767 (1996).
- [26] B. Cui, B. Lin, and S. A. Rice, *J. Phys. Chem.* **119**, 2386 (2003).